Absolute Heats of Formation of Phenylcarbene and Vinylcarbene

John C. Poutsma, John J. Nash, Jose A. Paulino, and Robert R. Squires*

Contribution from the Department of Chemistry, Purdue University, West Lafayette, Indiana 47907

Received November 12, 1996[⊗]

Abstract: The method of collision-induced dissociation threshold analysis for determining carbene thermochemistry is applied to the ground-state triplet carbenes CH_2 (methylene, **1**), CH_2═CHCH (vinylcarbene, **2**), and PhCH (phenylcarbene, **3**). The chief aims of this study are to evaluate the energetic and dynamical consequences of the obligatory curve-crossing that characterizes dissociation of a halide ion from an α-halocarbanion to form a carbene with a triplet ground state, and to determine accurate heats of formation for **2** and **3**. Threshold collision energies for loss of halide from CH_2X^- (X = Cl, Br), CH_2CHCHX^- (X = Cl, Br, I), and $PhCHX^-$ (X = Cl, Br, I) are determined with use of a flowing afterglow−triple quadrupole apparatus. The dissociation energies are combined with the measured gas-phase acidities of the corresponding methyl, allyl, and benzyl halides in simple thermochemical cycles in order to derive the absolute heats of formation for the carbenes. The value of $\Delta H_{f,298}$(**1**) derived from the results for the two different methyl halides (92.2 ± 3.7 kcal/mol) is in excellent agreement with the well-established literature value for the triplet ground state of methylene: $\Delta H_{f,298}[\tilde{X}\ ^3B_1\ CH_2] = 92.9 \pm 0.6$ kcal/mol. The good agreement indicates that dissociation of the halomethyl anions occurs adiabatically to produce the triplet state of the product without any significant reverse activation energy or dynamical constraints. The measured dissociation energies for 1-chloro-, 1-bromo-, and 1-iodoallyl anions are combined with the bracketed acidities of allyl chloride, bromide, and iodide to yield three independently determined but closely matched values for $\Delta H_{f,298}$(**2**): 92.3 ± 2.6, 93.9 ± 3.4, and 93.2 ± 3.1 kcal/mol, respectively. The average value from the three determinations, 93.3 ± 3.4 kcal/mol, is in fair agreement with the estimated heat of formation for the triplet ground state of **2** obtained from various MCSCF and density functional calculations (90 kcal/mol), but much lower than the predicted heat of formation for the lowest singlet state of **2** (100 kcal/mol). As with the halomethyl ions, efficient adiabatic dissociation of the haloallyl anions at the thermodynamic limit is indicated by these results. The apparent heats of formation for **3** derived from the measured dissociation energies for $PhCHCl^-$, $PhCHBr^-$ and $PhCHI^-$, and the bracketed acidities of the corresponding benzyl halides show a somewhat larger (non-systematic) variation, but are all within the assigned uncertainties. The derived values for $\Delta H_{f,298}$(**3**) are 103.2 ± 3.2, 105.5 ± 2.7, and 100.9 ± 2.8 kcal/mol for the benzyl chloride, bromide, and iodide systems, respectively, giving an average value of 102.8 ± 3.5 kcal/mol. The measured heats of formation for **2** and **3** are compared with the predictions obtained from various levels of ab initio theory. Density functional calculations with the BVWN5 and B3LYP functionals in conjunction with polarized, triple-ζ basis sets are found to perform best with respect to the singlet−triplet splittings and absolute heats of formation, while MCSCF and CISD methods lead to S−T gaps and heats of formation that are too high. The experimental thermochemistry is used to derive values for the α-CH bond strengths in allyl radical and benzyl radical: DH_{298}-$[CH_2$═$CHCH-H] = 104.0 \pm 3.4$ kcal/mol and $DH_{298}[PhCH-H] = 105.2 \pm 3.5$ kcal/mol.

Understanding the effects of different substituents on the electronic structures, reactivity, and relative stabilities of carbenes is a venerable pursuit of physical organic chemistry.[1] Experiment and theory have shown that the ground-state multiplicity and singlet−triplet splitting of a carbene are exquisitely sensitive to the nature of the substituents appended to the divalent carbon.[2] Singlet ground states are generally observed or predicted for carbenes possessing electronegative, π-donor substituents such as halogens, alkoxy, and amino groups, and for carbenes incorporated into small rings (cycloalkylidenes) and double bonds (vinylidenes). Triplet ground states are found for carbenes with electropositive groups or unsaturated, π-acceptor substituents such as cyano, phenyl, and vinyl. The multiplicity of the ground state and magnitude of the singlet−triplet splitting serve as the basis for the valence-state promotion energy models for carbene stability originally proposed by Carter and Goddard,[3] and recently extended by Chen and co-workers.[4] Thus, an important connection exists between substituent effects on the electronic structures and the thermochemistry of carbenes.

We have been developing gas-phase experimental methods for determining absolute heats of formation for carbenes based on the energetics of halide dissociation from α-halocarbanions (eq 1, X = F, Cl, Br, I). We use energy-resolved collision-

$$R_2CX^- \rightarrow R_2C: + X^- \qquad (1)$$

induced dissociation (CID) in a flowing afterglow−triple

[⊗] Abstract published in *Advance ACS Abstracts,* May 1, 1997.

(1) (a) Kirmse, W. *Carbene Chemistry*; Academic Press: New York, 1971. (b) Jones, M.; Moss. R. A. *Carbenes I*; Wiley: New York, 1973. (c) Jones, M.; Moss. R. A. *Carbenes II*; Wiley: New York, 1975. (d) Regitz, M. *Angew. Chem., Int. Ed. Engl.* **1991**, *30*, 674.

(2) (a) Hoffmann, R.; Zeiss, G. D.; Van Dine, G. W. *J. Am. Chem. Soc.* **1967**, *90*, 1485. (b) Baird, N. C.; Taylor, K. F. *J. Am. Chem. Soc.* **1978**, *100*, 1333. (c) Bauschlicher, C. W.; Schaefer, H. F., III; Bagus, P. S. *J. Am. Chem. Soc.* **1977**, *99*, 7106. (d) Harrison, J. F.; Liedtke, R. C.; Liebman, J. F. *J. Am. Chem. Soc.* **1979**, *101*, 7162. (e) Liebman, J. F.; Simons, J. In *Molecular Structure and Energetics*; Liebman, J. F., Greenberg, A., Eds.; VCH Publishers Inc.: Deerfield Beach FL, 1986; Vol. 1, Chapter 3.

(3) Carter, E. A.; Goddard, W. A., III. *J. Phys. Chem.* **1986**, *90*, 998. See also: Simons, J. *Nature* **1965**, *205*, 1308.

(4) Blush, J. A.; Clauberg, H.; Kohn, D. W.; Minsek, D. W.; Zhang, X.; Chen, P. *Acc. Chem. Res.* **1992**, *25*, 385.

S0002-7863(96)03918-2 CCC: $14.00

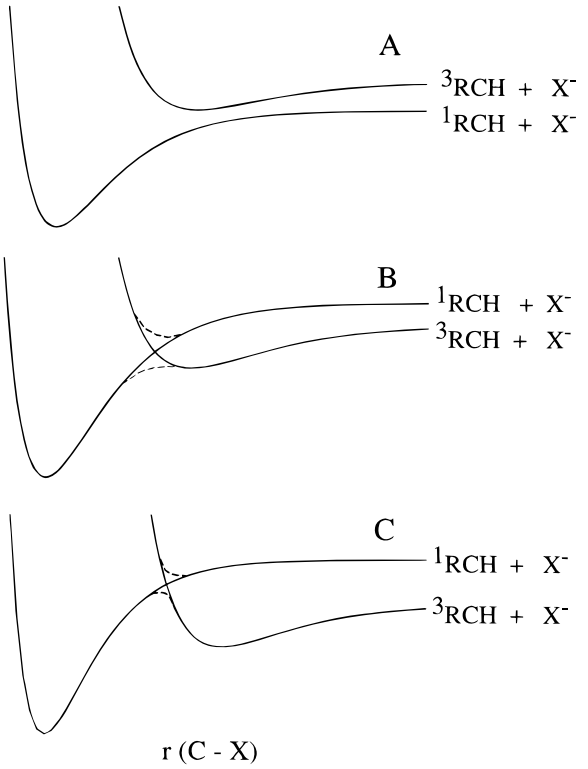

Figure 1. Schematic potential energy surfaces involved in dissociation of α-halocarbanions to carbenes: (A) ground-state singlet carbene; (B) ground-state triplet carbene with surface crossing occurring at an energy below the triplet asymptote, and (C) ground-state triplet carbene with surface crossing occurring at an energy above the triplet asymptote.

quadrupole instrument to determine the threshold energy for halide loss. The measured dissociation energy can be combined with the known[5] (or measurable) heats of formation of the reactant and product ions to determine the heat of formation for the carbene product. For systems involving *singlet* carbene products, dissociation on a single diabatic potential energy surface gives the ground state of the product directly (Figure 1A). The reverse process, nucleophilic addition to a singlet carbene, has been examined experimentally and computationally for simple cases and has been shown to occur without a barrier.[6] Thus, for singlet carbene systems the measured dissociation activation energies can be directly equated with the bond dissociation energies. In the first application of this experimental approach to the archetypal singlet carbenes CF_2 and CCl_2, excellent agreement was obtained between the measured heats of formation and literature values derived from different experimental methods and/or reliable ab initio calculations.[7] Analogous measurements with CHF, CHCl, and CFCl have been performed which give heats of formation that are also in good agreement with other determinations and with high-level calculations.[8]

Halocarbanion dissociations that produce carbenes with *triplet* ground states necessarily involve a surface-crossing, since the triplet carbene/halide ion surface is largely repulsive (Figure 1, parts B and C). If the intersystem-crossing rate is fast compared to halide dissociation, then adiabatic dissociation will give the ground-state triplet carbene product. However, the measured activation energy will depend upon the actual location of the crossing relative to the triplet asymptote, and the extent of mixing at this point. Therefore, a reverse activation energy is possible for this type of dissociation (Figure 1C). In general, we can expect that electrostatic interactions between the halide ion and the triplet carbene will decrease the energy of the dissociation barrier somewhat, but we have no guarantees that it will be below the triplet product asymptote (Figure 1B).[9]

In the present work we examine the energetics and dynamics of halide dissociation from three different types of α-halocarbanion that produce carbenes with triplet ground states (eqs 2−4, X = Cl, Br, I).

$$\underset{\mathbf{1}}{CH_2X^-} \rightarrow CH_2 + X^- \quad (2)$$

$$\underset{\mathbf{2}}{CH_2CHCHX^-} \rightarrow CH_2CHCH + X^- \quad (3)$$

$$\underset{\mathbf{3}}{PhCHX^-} \rightarrow PhCH + X^- \quad (4)$$

Methylene (**1**), the product of halide dissociation from a halomethyl anion, has an accurately known heat of formation and singlet−triplet splitting: $\Delta H_{f,298}[\tilde{X}\ ^3B_1\ CH_2] = 92.9 \pm 0.6$ kcal/mol, $\Delta E_{ST} = 9.0 \pm 0.1$ kcal/mol.[10−12] This system can therefore serve as a benchmark for evaluating the utility of CID threshold measurements for deriving triplet carbene thermochemistry. The triplet ground state ($^3A''$) predicted by theory for vinylcarbene (**2**) has been confirmed by ESR spectroscopy.[13] Photolysis of vinyldiazomethane in a glassy matrix at 6 K gives rise to two similar but non-identical signals with the hyperfine parameters: $D_{cis} = 0.4578$ cm^{-1}, $E_{cis} = 0.0193$ cm^{-1}, $D_{trans} = 0.4093$ cm^{-1}, and $E_{trans} = 0.0224$ cm^{-1}, which are assigned to the *cis* and *trans* geometric isomers of planar **2**, respectively. Davis *et al*. carried out generalized valence bond (GVB) calculations to characterize the ring-opening reaction of cyclopropene to vinylcarbene.[14] The *cis* and *trans* forms of ground-state $^3A''$ vinylcarbene were found to be nearly isoenergetic, lying 12 kcal/mol below the lowest planar singlet state, $\tilde{a}\ ^1A'$. Extensive MCSCF and multi-reference-CI calculations of the C_3H_4 potential energy surface carried out by Yoshimine and co-workers give similar results.[15] Phenylcarbene (**3**) has been the subject of several experimental[16] and theoretical[17−22] investigations. The planar $^3A''$ ground state for **3** predicted by theory has also been verified by low-temperature ESR studies, which give the hyperfine splitting parameters $D = 0.518$ cm^{-1}

(5) Lias, S. G.; Bartmess, J. E.; Liebman, J. F.; Holmes, J. L.; Levin, R. D.; Mallard, W. D. *J. Phys. Chem. Ref. Data* **1988**, *17*, Suppl. 1. All data taken from the NIST Negative Ion Energetics Database, Version 3.00, NIST Standard Reference Database 19B, October 1993.

(6) (a) Hack, W.; Wagner, H. G.; Wilms, A. *Ber. Bunsenges. Phys. Chem.* **1988**, *92*, 620. (b) Trinquier, G.; Malrieu, J. *J. Am. Chem. Soc.* **1979**, *101*, 7169. (c) Harding, L. B.; Schlegel, H. B.; Krishnan, R.; Pople, J. A. *J. Phys. Chem.* **1980**, *84*, 3394.

(7) Paulino, J. A.; Squires, R. R. *J. Am. Chem. Soc.* **1991**, *113*, 5573.

(8) (a) Poutsma, J. C.; Paulino, J. A.; Squires, R. R. *J. Phys. Chem.* In press. For preliminary values, see: Paulino, J. A.; Squires, R. R. *J. Am. Chem. Soc.* **1991**, *113*, 1845. Paulino, J. A. Ph.D. Thesis, Purdue University, 1992.

(9) Armentrout, P. B.; Simons, J. *J. Am. Chem. Soc.* **1992**, *114*, 8627.

(10) Leopold, D. G.; Murray, K. K.; Stevens-Miller A. E.; Lineberger, W. C. *J. Chem. Phys.* **1985**, *83*, 4849.

(11) (a) Lengel, R. K.; Zare, R. N. *J. Am. Chem. Soc.* **1978**, *100*, 7495. (b) Feldman, D.; Meier, K.; Zacharias, H.; Welge, K. H. *Chem. Phys. Lett.* **1978**, *59*, 171. (c) Hayden, C. C.; Neumark, D. M.; Shabatake, K.; Sparks, R. K.; Lee, Y. T. *J. Chem. Phys.* **1982**, *76*, 3607.

(12) (a) Petersson, G. A.; Al-Laham, M. A. *J. Am. Chem. Soc.* **1989**, *111*, 1256 and references therein (b) Schaefer, H. F., III *Science* **1986**, *231*, 1100. (c) Goddard, W. A., III *Science* **1985**, *227*, 917. (d) Shavitt, I. *Tetrahedron* **1985**, *41*, 1531.

(13) Hutton, R. S.; Manion, M. L.; Roth, H. D.; Wasserman, E. *J. Am. Chem. Soc.* **1974,** *96*, 4680.

(14) Davis, J. H.; Goddard, W. A., III; Bergman, R. G. *J. Am. Chem. Soc.* **1977**, *99*, 2427.

(15) (a) Honjou, N.; Pacansky, J.; Yoshimine, M. *J. Am. Chem. Soc.* **1985**, *107*, 5332. (b) Yoshimine, M.; Pacansky, J.; Honjou, N. *J. Am. Chem. Soc.* **1989**, *111*, 2785. (c) Yoshimine, M.; Pacansky, J.; Honjou, N. *J. Am. Chem. Soc.* **1989**, *111*, 4198.

and $E = 0.024$ cm^{-1}.[16a] Ab initio and DFT calculations on phenylcarbene recently reported by four different groups[19−22] suggest values for the singlet−triplet splitting ($\tilde{X}\ ^3A'' \rightarrow \tilde{a}\ ^1A'$) in **3** of about 4 kcal/mol, which is consistent with indirect experimental estimates.[23]

In the following, we first describe measurements of the dissociation energies of the halomethyl anions CH_2Cl^- and CH_2Br^- (eq 2), and a derivation of the absolute heat of formation for CH_2. The results for both systems are shown to be in good agreement with the known thermochemistry for triplet methylene. The formation, absolute basicities, and collision-induced dissociation of a series of 1-haloallyl and α-halobenzyl carbanions with X = Cl, Br, I are then described (eqs 3 and 4). Arguments are presented to support the assignment of vinylcarbene and phenylcarbene, respectively, as the threshold dissociation products. The same heat of formation for vinylcarbene is obtained from the results for the three different 1-haloallyl anions. Similarly, the apparent heats of formation for PhCH derived from measurements with three different halobenzyl anions agree within experimental error. Values for the α-CH bond strengths in allyl radical and benzyl radical are derived from the experimental thermochemistry, which allows an assessment of the sequential C-H bond energies of propene and toluene, respectively. Ab initio molecular orbital and DFT calculations of the geometries, singlet−triplet splittings, and absolute thermochemistry of vinylcarbene and phenylcarbene are also described, and compared with the experimental results.

Experimental Section

All experiments were carried out at room temperature (298 ± 2 K) with a flowing afterglow−triple quadrupole instrument that has been described in detail previously.[24] The standard operating conditions were P(He) = 0.40 Torr, F(He) = 190 STP cm^3/s, and v(He) = 9400 cm/s. The halocarbanions were produced by proton abstraction from the corresponding halocarbons by OH^- and, in the case of the halomethyl ions, by fluoride-induced desilylation of Me_3SiCH_2X compounds.[25] Hydroxide ion was generated by electron ionization of a mixture of N_2O and CH_4, and F^- was generated by ionization of NF_3. All ions in the flow reactor are thermalized by *ca.* 10^5 collisions with the He buffer gas prior to sampling through a small orifice into the low-pressure analyzer chamber. For collision-induced dissociation (CID) studies, the halocarbanions were mass-selected with the first quadrupole of the EXTREL triple quadrupole analyzer and then injected into the gas-tight, rf-only quadrupole (Q2) with a nominal lab-frame energy determined by the Q2 rod offset voltage. Argon and neon were used as collision gases in Q2 at low pressures corresponding to single-collision conditions (<0.05 mTorr). Fragment ions produced by CID were extracted into the third quadrupole, which was held at a constant attractive voltage (2−5 V) relative to Q2. Ion detection was carried out with a conversion dynode and an electron multiplier operating in pulse counting mode.

Energy Threshold Measurements. The general procedures used to measure energy-resolved CID data and to derive the threshold energy are described in detail elsewhere.[26−28] An appearance curve is generated from the energy-dependent ion abundances by plotting the partial cross section for formation of a particular fragment ion as a function of the center-of-mass (CM) collision energy of the mass-selected reactant ion. The CM collision energy is related to the nominal lab-frame energies, E_{lab}, by $E_{CM} = E_{lab}[m/(m + M)]$, where m and M are the masses of the neutral target and reactant ion, respectively. Absolute cross sections for formation of a single product ion from CID (σ_p) are calculated from the relation $\sigma_p = I_p/INl$, where I_p and I are the intensities of the product and reactant ions, N is the number density of the target gas, and l is the effective collision path length (24 ± 4 cm).[24]

The activation energy for dissociation is derived by fitting the experimental ion appearance curve with an assumed model function[29] that explicitly accounts for the reactant ion internal energy and unimolecular decomposition lifetime effects.[30] This function is given in eq 5, where E_T is the energy threshold, σ_o is a scaling factor, n is an

$$\sigma(E) = \sigma_o \sum_I [g_i P_D(E,E_i,\tau)(E + E_i - E_T)^n/E] \qquad (5)$$

adjustable parameter, and I denotes vibrational states of the reactant ion having energy E_i and population g_i ($\sum g_i = 1$). The vibrational internal energy distributions of the reactant ions were estimated from calculated harmonic frequencies obtained from semiempirical molecular orbital calculations.[31] The P_D term in eq 5 is the probability that the metastable reactant ion having internal energy ($E + E_i$) will dissociate within the (typical) flight-time of an ion from Q2 to the detector (*ca.* 30 μs).[24] This probability is estimated by performing RRKM calculations of the reactant ion decay rate as a function of internal energy (*vide infra*).[32] The parameters E_T, σ_o, and n are varied iteratively so as to minimize deviations between the experimental cross sections and the calculated values in the steeply rising portion of the appearance curve.[33] Convoluted into the fit are a Doppler broadening function developed by Chantry[34] and the reactant ion kinetic energy distribution, which is approximated by a Gaussian function with a full-width at half-maximum of 1.5 eV (lab).

In deriving the dissociation probability factors (P_D) from RRKM analysis of the activated halocarbanion lifetimes, some assumptions are required regarding the nature of the dissociation transition state. The relative "tightness" or "looseness" of the dissociation transition state is reflected by the activation entropy, $\Delta S^‡$, which can be estimated from the vibrational partition functions for the reactant ion (Q) and transition state ($Q^‡$) as in eq 6, where $q_i = 1/[\,1 - \exp(-h\nu/k_BT)]$, $E_v^‡$ and E_v are the average vibrational energies of the transition state and reactant ion, respectively, and k_B is the Boltzmann constant. By convention, the activation entropy is evaluated at 1000 K; values of $\Delta S^‡_{1000}$ are negative for tight transition states and positive for loose

(16) (a) Trozzolo, A. M.; Murray, R. W.; Wasserman, E. *J. Am. Chem. Soc.* **1962**, *84*, 4990. (b) Barash, L.; Wasserman, E.; Yager, W. A. *J. Am. Chem. Soc.* **1967**, *89*, 3931. (c) Becker, R. S.; Bost, R. O.; Kolc, J.; Bertoniere, N. R.; Smith, R. L.; Griffin, G. W. *J. Am. Chem. Soc.* **1970**, *92*, 1302. (d) Savino, T. G.; Kanakarajan, K.; Platz, M. S. *J. Org. Chem.* **1986**, *51*, 1305.

(17) Radom, L; Schaefer, H. F., III; Vincent, M. A. *Nouv. J. Chim.* **1980**, *4*, 411.

(18) (a) Li, Y.-Z.; Schuster, G. B. *J. Org. Chem.* **1988**, *53*, 1273. (b) Dannenburg, J. J.; Vinson, L. K.; Moreno, M.; Bertran, J. *J. Org. Chem.* **1989**, *54*, 5487. (c) Karaman, R.; Huang, J.-T. L.; Fry, J. L. *J. Comp. Chem.* **1991**, *5*, 536.

(19) Cramer, C. J.; Dulles, F. J.; Falvey, D. E. *J. Am. Chem. Soc.* **1994**, *116*, 9787.

(20) Matzinger, S.; Bally, T.; Patterson, E. V.; McMahon, R. J. *J. Am. Chem. Soc.* **1996**, *118*, 1535.

(21) Wong, M. W.; Wentrup, C. *J. Org. Chem.* **1996**, *61*, 7022.

(22) Schreiner, P. R.; Karney, W. L.; Schleyer, P. v. R.; Borden, W. T.; Hamilton, T. P.; Schaefer, H. F. *J. Org. Chem.* **1996**, *61*, 7030.

(23) Platz, M. S. *Acct. Chem Res.* **1995**, *28*, 487 and references therein.

(24) Marinelli, P. J.; Paulino, J. A.; Sunderlin, L. S.; Wenthold, P. G.; Poutsma, J. C.; Squires, R. R. *Int. J. Mass Spec. Ion Proc.*, **1994**, *130*, 89.

(25) DePuy, C. H.; Bierbaum, V. M.; Flippin, L. A.; Grabowski, J. J.; King, G. K.; Schmitt, R. J.; Sullivan, S. A. *J. Am. Chem. Soc.* **1980**, *102*, 5012.

(26) (a) Sunderlin, L. S.; Wang, D.; Squires, R. R. *J. Am. Chem. Soc.* **1992**, *114*, 2788. (b) Sunderlin, L. S.; Wang, D.; Squires, R. R. *J. Am. Chem. Soc.* **1993**, *115*, 12060.

(27) Wenthold, P. G.; Squires, R. R. *J. Am. Chem. Soc.* **1994**, *116*, 6961.

(28) (a) Wenthold, P. G.; Wierschke, S. G.; Nash, J. J.; Squires R. R. *J. Am. Chem. Soc.* **1993**, *115*, 12611. (b) Wenthold, P. G.; Wierschke, S. G.; Nash, J. J.; Squires, R. R. *J. Am. Chem. Soc.* **1994**, *116*, 7378.

(29) (a) Chesnavich, W. J.; Bowers, M. T. *J. Phys. Chem.* **1979**, *83*, 900. (b) Sunderlin, L. S.; Armentrout, P. B. *Int. J. Mass Spectrom. Ion Processes* **1989**, *94*, 149.

(30) (a) Schultz, R. H.; Crellen, K. C.; Armentrout, P. B. *J. Am. Chem. Soc.* **1991**, *113*, 8590. (b) Khan, F. A.; Clemmer, D. E.; Schultz, R. H.; Armentrout, P. B. *J. Phys. Chem.* **1993,** *97*, 7978.

(31) AM1: Dewar, M. J. S.; Zoebisch, E. G.; Healy, E. F.; Stewart, J. J. P. *J. Am. Chem. Soc.* **1985**, *107*, 3902. MOPAC: Stewart, J. J. P. QCPE No. 455.

(32) (a) Robinson, J. P.; Holbrook, K. A. *Unimolecular Reactions*; Wiley-Interscience: New York, 1972. (b) Forst, W. *Theory of Unimolecular Reactions*; Academic: New York, 1973.

(33) Analysis carried out using the CRUNCH program developed by P. B. Armentrout and K. M. Ervin.

(34) Chantry, P. J. *J. Chem. Phys.* **1971**, *55*, 2746.

$$\Delta S^{\ddagger} = k_B \ln(Q^{\ddagger}/Q) + (E_v^{\ddagger} - E_v)/T = k_B \ln(\prod q_i^{\ddagger}/\prod q_i) + (E_v^{\ddagger} - E_v)/T \quad (6)$$

transition states.[35] As in the previous studies of collisionally-activated halide elimination reactions of *o*-, *m*- and *p*-halophenyl anions[27] and halobenzyl anions,[28] we assume "product-like" transition states for the α-halocarbanion dissociations that are characterized by the vibrational frequencies of the product carbene plus two additional low frequencies near 25 cm^{-1} to represent in-plane and out-of-plane bending of the dissociating carbon−halide bond.[36] This particular choice of bending frequencies gives $\Delta S^{\ddagger}_{1000}$ values for the halocarbanion dissociations in the range 4−8 eu. This same range for $\Delta S^{\ddagger}_{1000}$ was used in the energy-resolved CID studies of halophenyl and halobenzyl anions.

For a dissociation reaction with no reverse activation energy, the threshold value, E_T, derived from the above analysis corresponds to the 0 K bond dissociation energy, ΔE_o. The corresponding 298 K enthalpy change, DH_{298}, is obtained from ΔE_o by adding the difference in 0−298 K integrated heat capacities for the products and reactants and a factor of *RT* (0.59 kcal/mol at 298 K) to represent the PV work for dissociation. The thermochemical results reported in this work employ the "stationary electron" convention.[5]

Materials. Gas purities were as follows: He (99.995%), Ar (99.955%), Ne (99.99%), N_2O (99%), CH_4 (99%), NF_3 (99%). All reagents were obtained from commercial sources and used as supplied except for degassing of liquid samples prior to use.

Computational Details. Optimized geometries for the singlet and triplet states of methylene (**1**), vinylcarbene (**2**), phenylcarbene (**3**), and the corresponding hydrocarbons methane, propene, and toluene were obtained by MCSCF(*n*,*n*) calculations with a 3-21G basis set, using active orbital spaces that included all π-type orbitals in each molecule along with the in-plane σ orbital for each carbene. The following procedures and symmetry constraints were employed: methylene MCSCF(2,2)/3-21G (C_{2v}), vinylcarbene MCSCF(4,4)/3-21G (C_s), phenylcarbene MCSCF(8,8)/3-21G (C_s), methane HF/3-21G (T_d), propene MCSCF(2,2)/3-21G (C_s), and toluene MCSCF(6,6)/3-21G (C_s).

All optimized structures were verified to be minima within the defined symmetry by the absence of any negative eigenvalues in the Hessian matrices derived from frequency calculations carried out with the MCSCF and HF procedures identified above. For the MCSCF vibrational analysis, numerically-evaluated energy gradients were used. Zero-point energies (ZPE) were computed from the scaled harmonic frequencies (scale factor = 0.9[37]) obtained from MCSCF(2,2)/6-31G* calculations[38] for the carbenes and HF/6−31G* calculations for the closed-shell hydrocarbons.

Total energies for the three carbenes, methane, propene, and toluene, were also computed at the MCSCF(*n*,*n*) and CISD levels with use of the Dunning polarized, correlation-consistent [9s4p1d/3s2p1d] double-ζ basis set for carbon (including 6 d functions) and a [4s/2s] basis set for hydrogen[39,40] at the MCSCF(*n*,*n*)/3-21G geometries. This basis set is designated cc-pVDZ although it lacks polarization functions on the hydrogen atoms. The CISD calculations for the carbenes employed a single reference configuration for each triplet state and two reference configurations for each singlet state, which were constructed from the natural orbitals resolved from the corresponding MCSCF(*n*,*n*)/cc-pVDZ calculations. All symmetry-allowed single and double excitations from the reference configuration(s) were included, except for those from the non-valence molecular orbitals (frozen core approximation). The CISD energies obtained in this way were corrected for the estimated effects of quadruple excitations by the method of Davidson (i.e., CISD+DV2).[41] Total energies for the MCSCF(*n*,*n*)/3-21G geometry of each species were also determined from density functional theory by using two different exchange-correlation functional combinations: the Becke exchange functional[42] with the V correlation functional of Vosko, Wilk, and Nusair (BVWN5),[43] and the Becke three-parameter exchange functional[44] with the correlation functional of Lee, Yang and Parr[45] (B3LYP). Both sets of calculations employed the Dunning polarized, correlation-consistent [10s5p2d1f/4s3p2d1f] (6 d functions) triple-ζ basis set[39] (i.e., BVWN5/cc-pVTZ and B3LYP/cc-pVTZ).

The HF and DFT calculations were carried out with use of the Gaussian 92/DFT[46] suite of programs, and the MCSCF and CISD calculations were performed by using either the Gaussian 92/DFT or MOLCAS programs.[47]

Results

The absolute heat of formation of the carbene product of a halocarbanion dissociation reaction (eqs 2−4) can be expressed in terms of the dissociation enthalpy, $DH_{298}[RCH-X^-]$, and the gas-phase acidities and heats of formation for RCH_2X and HX (eq 7).

$$\Delta H_{f,298}(RCH) = DH_{298}[RCH-X^-] + \Delta H_{acid}(RCH_2X) + \Delta H_{f,298}(RCH_2X) - \Delta H_{acid}(HX) - \Delta H_{f,298}(HX) \quad (7)$$

The dissociation enthalpy can be derived from the measured threshold energy for halide loss from the collisionally-activated halocarbanion, provided that dissociation occurs rapidly on the instrument time scale with no reverse activation energy. The auxiliary thermochemical data for HX and RCH_2X indicated in eq 7 are available in the literature[5] or can be estimated by additivity methods.[48] The values used in this study are listed in Table 1. The gas-phase acidities of the methyl, allyl, and benzyl halides, $\Delta H_{acid}(RCH_2X)$, are either known or can be measured *via* equilibrium or bracketing techniques.

One advantage of the present approach to carbene thermochemistry is that it permits multiple independent measurements of the heat of formation of the carbene by use of different halocarbanion precursors. That is, heats of formation derived from eq 7 with X = F, Cl, Br, and I should all be the same, provided that each different halocarbanion dissociates at the thermodynamic limit and the auxiliary thermochemical data are accurately known. Systematic variations in the results obtained with different halides could signal the presence of a reverse activation energy or some dynamical constraint that invalidates the presumption of thermodynamic control for the dissociation.

(35) Lifshitz, C. *Adv. Mass Spectrom.* **1989**, *7*, 713.

(36) Bending frequencies were obtained by loosening the carbon−halide bending modes in the reactant anions by factors between 2 and 10. Threshold curves were fit with assumed transition states corresponding to activation entropies that were 2 eu higher and 2 eu lower than the ones used in the final analysis. The effect on the threshold energies was less than or equal to 1 kcal/mol for all three halobenzyl anion dissociations.

(37) We employed an average scale factor of 0.9 because some of the calculated frequencies were analytically derived while others were numerically evaluated. This value is in the range of the one recommended by Pople and Radom for HF/6-31G* frequencies. Pople, J. A.; Scott, A. P.; Wong, M. W.; Radom, L. *Isr. J. Chem.* **1993**, *33*, 345.

(38) The active orbital spaces for these calculations consisted of the nonbonding σ and π orbitals of each carbene. A single reference configuration was used for the triplet states (i.e., ROHF/6-31G*), and a two-configuration reference was used for each singlet state (i.e. TCSCF/6-31G*).

(39) Dunning, T. H. *J. Chem. Phys.* **1989**, *90*, 1007.

(40) (a) Dunning, T. H. *J. Chem. Phys.* **1970**, *53*, 2823. (b) Dunning, T. H. *J. Chem. Phys.* **1971**, *55*, 716.

(41) (a) Langhoff, S. R.; Davidson, E. R. *Int. J. Quantum Chem* **1974**, *8*, 61. (b) Blomberg, M. R. A.; Siegbahn, P. E. M. *J. Chem. Phys.* **1983**, *78*, 5682.

(42) Becke, A. D. *J. Phys. A.* **1988**, *38*, 3098.

(43) Vosko, S. H.; Wilk, N.; Nusair, M. *Can. J. Phys.* **1980**, *58*, 1200.

(44) Becke, A. D. *J. Chem. Phys.* **1993**, *98*, 5648.

(45) Lee, C.; Yang, W.; Parr, R. G. *Phys. Rev. B.* **1988**, *37*, 785.

(46) Gaussian 92/DFT Revision G.3; Frisch, M. J.; Trucks, G. W.; Schlengel, H. B.; Gill, P. M. W.; Johnson, B. G.; Wong, M. W.; Foresman, J. B.; Robb, M. A.; Head-Gordon, M.; Replogle, E. S.; Gomperts, R.; Andres, J. L.; Raghavachari, K.; Binkley, J. S.; Gonzalez, C.; Martin, R. L., Fox, D. J.; Defrees, D. J.; Baker, J.; Stewart, J. J. P.; Pople, J. A.; Gaussian, Inc.: Pittsburgh, PA, 1993.

(47) MOLCAS-2: Anderson, K.; Blomberg, M. R. A.; Fülscher, M. P.; Kellö, V.; Lindh, R.; Malmqvist, R.-Å.; Noga, J.; Olsen, J.; Roos, B. O.; Sadlej, A. J.; Siegbahn, P. E. M.; Urban, M.; Widmark, P.-O; University Lund: Sweden, 1992.

(48) (a) Benson, S. W. *Thermochemical Kinetics*; John Wiley & Sons: New York, 1976. (b) Benson, S. W.; Garland, L. J. *J. Phys. Chem.* **1991**, *95*, 4915.

Table 1. Supplemental and Thermochemical Data

compd	$\Delta H_{f,298}$(g), kcal/mol[a]	compd	$\Delta H_{f,298}$(g), kcal/mol[a]
CH_3Cl	-19.6 ± 0.1	CH_4	-17.8 ± 0.4[b]
CH_3Br	-9.1 ± 0.3	$CH_2{=}CHCH_3$	4.0 ± 0.7[c]
$CH_2{=}CHCH_2Cl$	-1.3 ± 0.6	$CH_2{=}CHCH_2$	41.4 ± 0.4[b]
$CH_2{=}CHCH_2Br$	11.4 ± 0.6	$C_6H_5CH_3$	12.0 ± 0.1[c]
$CH_2{=}CHCH_2I$	23.8 ± 0.6	$C_6H_5CH_2$	49.7 ± 0.6[b]
$C_6H_5CH_2Cl$	4.0 ± 0.7	$(^1A_1)\ CH_2$	101.8 ± 0.5[d]
$C_6H_5CH_2Br$	16.0 ± 0.5	$(^3B_1)\ CH_2$	92.9 ± 0.6[e]
$C_6H_5CH_2I$	25.0 ± 1.0		

compd	ΔH_{acid}, kcal/mol	compd	ΔH_{acid}, kcal/mol
HCl	333.4 ± 0.2	HI	314.4 ± 0.1
HBr	323.6 ± 0.3		

[a] All data from ref 5 unless otherwise noted. [b] Berkowitz, J.; Ellison, G. B.; Gutman, D. *J. Phys. Chem.* **1994,** 98, 2744. [c] Reference 72. [d] Reference 11. [e] Reference 10.

In the present study we have addressed this issue by examining two different halomethyl anions (X = Cl, Br) and three different haloallyl and halobenzyl anions (X = Cl, Br, I).

Methylene. Chloromethyl and bromomethyl anions (CH_2X^-, X = Cl, Br) were prepared by fluoride-induced desilylation of the corresponding halomethyltrimethylsilanes, as shown in eq 8. The major ionic product of both reactions is the corresponding halide ion, Cl^- and Br^-, formed either by nucleophilic displacement at carbon or by a dissociative rearrangement involving attack at silicon followed by methyl migration.[49]

$$(CH_3)_3SiCH_2X + F^- \rightarrow CH_2X^- + (CH_3)_3SiF$$
$$\rightarrow X^- + (CH_3)_3SiCH_2F \text{ or}$$
$$(CH_3)_2Si(F)CH_2CH_3 \qquad (8)$$

Collisional activation of CH_2Cl^- in the triple quadrupole analyzer with argon or neon target gas produces Cl^- as the only ionic product in the 1−30 eV (lab) collision energy range. A representative chloride ion appearance curve for CID with neon target gas is shown in Figure 2.[50] The maximal cross section for this reaction is 1.5 Å^2 at approximately 6 eV (CM). The feature near the origin (see inset) corresponds to formation of chloride ion by an exothermic reaction with unavoidable traces of oxygen impurity in the collision cell (eq 9).

$$CH_2Cl^- + O_2 \rightarrow Cl^- + CH_2O_2 \qquad (9)$$

Thermochemical estimates indicate that the neutral product of this reaction could be any one of the [C, 2H, 2O] isomers, including formic acid, dioxirane, or even formaldehyde *O*-oxide.[51] Control experiments were carried out in which different mixtures of O_2 and Ar were used as collision targets for energy-resolved CID of CH_2Cl^-. The cross sections measured at each value of the collision energy were then extrapolated to zero oxygen contaminant, and the resulting extrapolated appearance curve was fit with eq 5. The optimized values of E_T and n obtained from the extrapolated data were found to be essentially

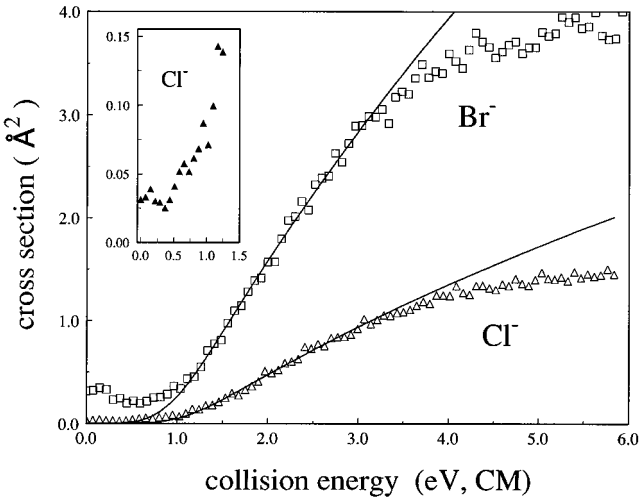

Figure 2. Cross sections for dissociation of halide ion from halomethyl anions resulting from collisional activation with neon target at *ca.* 3.0 × 10^{-5} Torr (eq 2). The solid lines are the optimized, fully convoluted model appearance curves obtained with use of eq 5 as described in the text. The small features near the collision energy origin (see inset) in both halide curves are due to exothermic reactions between the CH_2X^- ions and trace oxygen contaminant in the neon target gas (see text).

the same as those obtained by fitting the steeply-rising, post-threshold region of appearance curves in which the exothermic feature was minimized. This suggests that small amounts of oxygen impurity do not obscure the CID threshold analysis.

Analysis of the CID cross sections for CH_2Cl^- with and without the inclusion of the dissociation probability factors, P_D, in the model (eq 5) indicates a negligible influence of ion lifetime effects on the threshold behavior. The average internal energy content of CH_2Cl^- at 298 K based on the computed vibrational frequencies is 0.016 eV (0.4 kcal/mol), so this contribution to the CID cross section is also small. Analysis of multiple Cl^- appearance curves having minimal contaminant features gives average values for the fitting parameters E_T = 0.95 ± 0.13 eV (21.9 ± 2.9 kcal/mol) and n = 1.54 ± 0.10, where the uncertainty in E_T is derived from the precision of the measurements and a 0.15 eV (lab) (0.04 eV, CM) uncertainty in the energy scale. Combining this with the difference in 0−298 K integrated heat capacities between the CID products and reactants[52] and a PV = *RT* work term gives $DH_{298}[CH_2{-}Cl^-]$ = 23.1 ± 2.9 kcal/mol.

The energy-resolved CID behavior of bromomethyl anion, CH_2Br^-, is similar; a representative Br^- appearance curve is given in Figure 2. Bromide ion is the only ionic product formed by CID in the 0−30 eV energy range, and the maximum CID cross section is 4 Å^2 at about 4 eV (CM). The feature in the Br^- appearance curve due to O_2 contaminant in the neon target gas is more pronounced, but its influence on the threshold analysis is negligible. Ion lifetime effects are also insignificant in the observed CID cross sections, and the internal energy contribution (0.021 eV, 0.5 kcal/mol) is quite small. The average values of E_T and n obtained from replicate measurements are E_T = 0.87 ± 0.07 eV (20.1 ± 1.6) and n = 1.61 ± 0.07, where the uncertainty in E_T is determined as before by the precision of the measurements (±0.06 eV) and a 0.03 eV CM uncertainty in the energy scale. Converting this value for E_T to a 298 K enthalpy change in the prescribed manner gives $DH_{298}[CH_2{-}Br^-]$ = 21.1 ± 1.6 kcal/mol.

The thermochemical relation given by eq 7 for R = H and X = Cl, Br requires values for the gas-phase acidities (ΔH_{acid}) of

(49) Damrauer, R.; Danahey, S. E.; Yost, V. E. *J. Am. Chem. Soc.* **1984**, *106*, 7633.

(50) The energy-resolved cross section obtained with argon target is similar in appearance, although it displays somewhat more tailing in the threshold region. Because of the greater spread in the lab-frame collision energies when neon compared to argon target is used, the former is preferred for energy-resolved analysis of low-dissociation energy reactions.

(51) Kafafi, S. A.; Martinez, R. I.; Herron, J. T. In *Molecular Structure and Energetics*, Liebman, J. L., Greenberg, A., Eds.; VCH: Deerfield Beach, FL, 1988; Vol. 6.

(52) Translational and rotational contributions to the heat capacity are treated classically, and the vibrational components were obtained from calculated vibrational frequencies.

Table 2. Thermochemical Results for Methylene, Vinylcarbene, and Phenylcarbene

$RCHX^-$	E_T (eqs 2, 3, 4)[b]	n (eq 5)	$DH_{298}[RCH-X^-]$[b]	$\Delta H_{acid}(RCH_2X)$[b]	$\Delta H_{f,298}(RCH)$[b]
CH_2Cl^-	21.9 ± 2.9	1.54 ± 0.10	23.1 ± 2.9	400 ± 2	92.2 ± 3.9
CH_2Br^-	20.1 ± 1.6	1.61 ± 0.07	21.1 ± 1.6	395 ± 3	92.2 ± 3.4
					92.2 ± 3.7[a]
$CH_2{=}CHCHCl^-$	28.6 ± 1.6	1.52 ± 0.07	29.5 ± 1.6	375.4 ± 2.0	92.3 ± 2.6
$CH_2{=}CHCHBr^-$	21.2 ± 2.6	1.55 ± 0.08	22.0 ± 2.6	375.3 ± 2.0	93.9 ± 3.4
$CH_2{=}CHCHI^-$	18.7 ± 2.2	1.51 ± 0.08	19.5 ± 2.2	370.7 ± 2.0	93.2 ± 3.1
					93.3 ± 3.4[a]
$C_6H_5CHCl^-$	37.4 ± 2.4	1.68 ± 0.10	38.5 ± 2.4	372.0 ± 2.0	103.2 ± 3.2
$C_6H_5CHBr^-$	31.4 ± 1.7	1.53 ± 0.09	32.5 ± 1.7	371.7 ± 3.0	105.5 ± 3.5
$C_6H_5CHI^-$	24.2 ± 1.6	1.50 ± 0.10	24.9 ± 1.6	371.8 ± 2.0	100.9 ± 2.8
					102.8 ± 3.5[a]

[a] Pooled average of all measurements; see text for uncertainty assignment. [b] In units of kcal/mol.

methyl chloride and methyl bromide. Two independent measurements of both acidities are available in the literature. Ingemann and Nibbering report values of ΔH_{acid} for CH_3Cl and CH_3Br of 396.1 ± 3.1 and 392.8 ± 3.1 kcal/mol, respectively, which were obtained from acid−base bracketing measurements carried out in a Fourier transform ICR.[53] Hierl and Henchman determined threshold energies for endothermic proton transfer from CH_3Cl and CH_3Br to OH^- in an ion beam instrument and recommend the values $\Delta H_{acid}(CH_3Cl) = 399.6 \pm 2.5$ kcal/mol and $\Delta H_{acid}(CH_3Br) = 396.7 \pm 2.5$ kcal/mol.[54] The discrepancy between the ion beam results and the bracketed acidities is attributed by Hierl and Henchman to interfering side reactions (S_N2) in the ICR experiments. Ab initio molecular orbital calculations carried out at the G2 level of theory predict acidities for CH_3Cl and CH_3Br (ΔH_{acid} at 298 K) of 398.2 and 393.2 kcal/mol, respectively.[55] We have attempted to determine the equilibrium constant for proton transfer between chloromethyl anion and benzene ($\Delta H_{acid}(C_6H_6) = 401.7 \pm 0.5$ kcal/mol[56]), eq 10.

$$CH_2Cl^- + C_6H_6 \rightleftharpoons CH_3Cl + C_6H_5^- \qquad (10)$$

While it is clear that CH_2Cl^- reacts with benzene to produce some phenide anion, the major product ion (>98%) is Cl^-, which is presumably formed by nucleophilic displacement within the ion/molecule complex following proton transfer. Moreover, the yield of CH_2Cl^- from the reaction between phenide ion and CH_3Cl is less than 1%, the major product again being Cl^-. This behavior makes equilibrium analysis for reaction 10 unreliable. However, its occurrence as a reversible reaction is significant. On the basis of the ion beam results, the apparent reversibility of reaction 10, and the prediction from G2 theory, we assign $\Delta H_{acid}(CH_3Cl)$ to be 400 ± 2 kcal/mol. For methyl bromide we adopt the average of the Hierl and Henchman value and the value predicted by G2 theory, 395 ± 3 kcal/mol, with an uncertainty that encompasses both values. A summary listing of the acidities and CID threshold data for the methyl halides is given in Table 2.

Combining the dissociation enthalpies and acidities described above with the appropriate auxiliary data from Table 1 according to eq 7 gives two independent values for the 298 K heat of formation for methylene, $\Delta H_{f,298}(CH_2)$: 92.2 ± 3.9 from the methyl chloride results and 92.2 ± 3.4 kcal/mol from the methyl bromide results. The indicated uncertainties are determined from the root-square sums of the component uncertainties, and a major contributor in both cases is the uncertainty in the gas-phase acidity of the methyl halide. The agreement between these two values is excellent; pooling all data gives an average value for $\Delta H_{f,298}(CH_2)$ of 92.2 ± 3.7 kcal/mol. The absolute heats of formation for the triplet ground state and the (lowest) singlet excited state of methylene are well-established: $\Delta H_{f,298}[\tilde{X}\ ^3B_1\ CH_2] = 92.9 \pm 0.6$ kcal/mol and $\Delta H_{f,298}[\tilde{a}\ ^1A_1\ CH_2] = 101.9 \pm 0.5$ kcal/mol.[10−12] The good correspondence between the apparent heat of formation for methylene determined by energy-resolved CID and the known value for the triplet ground state indicates that dissociation of the collisionally-activated halomethyl anions occurs adiabatically with no excess energy barrier beyond the reaction endothermicity. It is implicit in this conclusion that the intersystem crossing required to produce CH_2 in its triplet state must be fast on the time scale of the halide dissociation.

Vinylcarbene. The 1-haloallyl anions CH_2CHCHX^- with X = Cl, Br, and I were produced in the flow reactor by proton abstraction from the corresponding allyl halides by OH^-.[57] The major primary product of these reactions is the corresponding halide ion, formed by substitution and/or elimination. Fast secondary reactions between the 1-haloallyl anions and the neutral allyl halides also produce the halide ions, thereby limiting the maximum abundances of the carbanions that can be achieved. Collisional activation of the 1-haloallyl anions in the 1−10 eV (CM) energy range with argon and neon targets yield the corresponding halide ions as the only ionic products (eq 3). The energy-resolved CID cross sections for the 1-chloro-, 1-bromo-, and 1-iodoallyl anions obtained with neon collision gas[50] are shown in Figure 3. No low-energy features due to O_2 contaminant in the target gas are observed in the haloallyl anion CID cross sections. The maximum CID cross sections range from *ca.* 3.5 to 10 Å^2, with the chloroallyl anion exhibiting the lowest cross section and the iodoallyl anion showing the highest.

The Cl^-, Br^-, and I^- appearance curves were modeled by using eq 5. As with the halomethyl anions, the dissociation probability factors for the haloallyl anions are found to be essentially unity at threshold, so there are no significant effects due to kinetic shifts in the CID onsets. The average internal energies of the CH_2CHCHX^- ions are estimated from the computed vibrational frequencies to be 1.4, 1.5, and 1.5 kcal/mol for X = Cl, Br, I, respectively, and there are several low-frequency modes in these ions such that the internal energy convolution makes a small but significant contribution to the CID cross section at the threshold. Average values for the fitting

(53) Ingemann, S.; Nibbering, N. M. M. *J. Chem. Soc., Perkin Trans. 2* **1985**, 837.

(54) Hierl, P. M.; Henchman, M. J. *Int. J. Mass Spectrom. Ion Processes* **1992**, *117*, 475.

(55) Methyl chloride: Smith, B. J.; Radom, L. *J. Phys. Chem.* **1991**, *95*, 10549. Methyl bromide: Mayer, P. A.; Radom, L. Personal communication of unpublished results.

(56) Davico, G. E.; Bierbaum, V. M.; DePuy, C. H.; Ellison, G. B.; Squires, R. R. *J. Am. Chem. Soc.* **1995**, *117*, 2590.

(57) The 1-bromoallyl anion was also generated by proton abstraction from 1-bromopropene; the behavior of the bromoallyl ions produced from the two different precursors is identical.

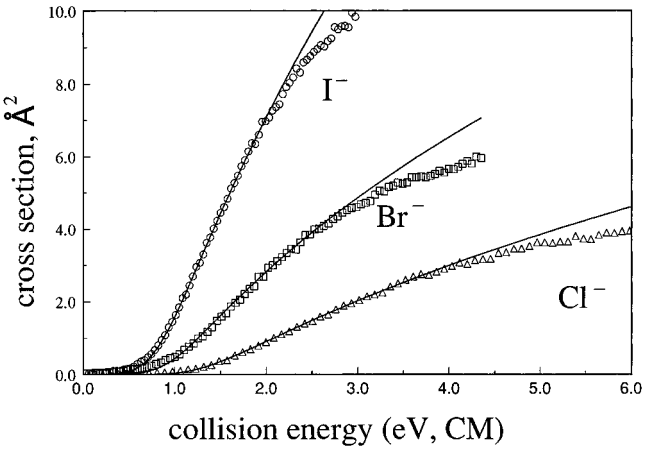

Figure 3. Cross sections for dissociation of halide ion from haloallyl anions resulting from collisional activation with neon target at *ca.* 3.0 $\times$ 10^{-5} Torr (eq 3). The solid lines are the optimized, fully convoluted model appearance curves obtained with use of eq 5 as described in the text.

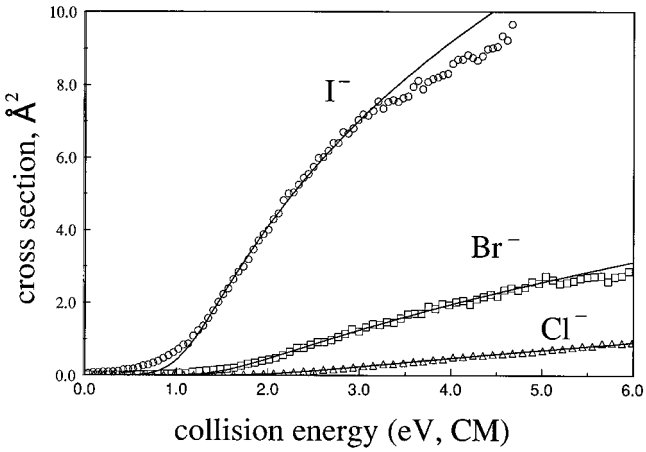

Figure 4. Cross sections for dissociation of halide ion from halobenzyl anions resulting from collisional activation with argon target at *ca.* 3.0 $\times$ 10^{-5} Torr (eq 4). The solid lines are the optimized, fully convoluted model appearance curves obtained with use of eq 5 as described in the text.

parameters E_T and n obtained from replicate measurements of the halide appearance curves for each of the three haloallyl anions are listed in Table 2, where the uncertainties are determined in the manner described previously. The corresponding 298 K enthalpy changes for reaction 3 are determined by applying the appropriate temperature corrections and a RT factor to each E_T value.

The gas-phase acidities of each of the allyl halides were determined by bracketing experiments, wherein a series of anionic reference bases with known proton affinities were allowed to react with each allyl halide. The reverse reaction, proton transfer to the haloallyl anions by reference acids, was not examined because of the uncertainty in the site of protonation (the 1- or 3-position) of these unsymmetrical allylic species.[58] The bracketing results are given in tabular form in the Supporting Information. Allyl chloride and allyl bromide behave identically, in that proton transfer occurs to *i*-PrO$^-$ (ΔG_{acid}(*i*-PrOH) = 370.1 $\pm$ 0.6 kcal/mol)[59] and to each of the stronger base anions that were examined, while no proton transfer occurs to F$^-$ (ΔG_{acid}(HF) = 365.1 $\pm$ 0.3 kcal/mol)[5] or any of the weaker bases. Proton abstraction by *t*-BuO$^-$ (ΔG_{acid}(*t*-BuOH) = 369.3 $\pm$ 0.6 kcal/mol)[59] appears to be relatively slow, as indicated by the significantly greater flow rates of the neutral allyl halides that are required to deplete the *t*-BuO$^-$ ion signal. In contrast, allyl iodide reacts by proton transfer to *t*-BuO$^-$ with noticeably greater efficiency, and it also transfers a proton to F$^-$, CH_2CN^- ($\Delta G_{acid}(CH_3CN)$ = 365.2 $\pm$ 2.0 kcal/mol),[5] and $FCH_2CH_2O^-$ ($\Delta G_{acid}(FCH_2CH_2OH)$ = 363.5 $\pm$ 3.5 kcal/mol).[60] In each of these reactions, the major observed product is the corresponding halide ion, Cl$^-$, Br$^-$, and I$^-$, formed by nucleophilic substitution or elimination. From these results, we assign values for the acidities of the allyl halides, ΔG_{acid}(CH_2=$CHCH_2X$), to be 368.0 $\pm$ 2.0, 368.0 $\pm$ 2.0, and 363.4 $\pm$ 2.0 kcal/mol for X = Cl, Br, and I, respectively. The corresponding enthalpy term, ΔH_{acid}(CH_2=$CHCH_2X$), can be calculated by using $\Delta H_{acid} = \Delta G_{acid} + T\Delta S_{acid}$, where ΔS_{acid} is the entropy change for acid dissociation given by $\Delta S_{acid} = S(H^+) + S(C_3H_4X^-) - S(C_3H_5X)$.[61] The absolute entropy of a proton, $S(H^+)$, is accurately known to be 26.0 eu,[62] and the absolute entropies of C_3H_5X and $C_3H_4X^-$ can be estimated by using standard statistical mechanical formulae.[63] The molecular vibrational frequencies and rotational constants needed for these estimates were obtained from semiempirical molecular orbital calculations[31] of the structures and normal modes of each of the allyl halides and haloallyl anions. For the three allyl halides, the resulting values for ΔS_{acid} are 24.7, 24.5, and 24.6 eu for X = Cl, Br, and I, respectively. Therefore, at 298 K ΔH_{acid}(CH_2=$CHCH_2X$) = 375.4 $\pm$ 2.0, 375.3 $\pm$ 2.0, and 370.7 $\pm$ 2.0 kcal/mol for X = Cl, Br, and I, respectively (Table 2). The value for ΔH_{acid}(CH_2=$CHCH_2Cl$) obtained in the present study is considerably lower than, but within the uncertainty of, the acidity given by Dahlke and Kass[64] (379.0 $\pm$ 4.0 kcal/mol). The higher value was determined by a bracketing procedure to be between that for CH_3OH and CH_3CH_2OH.

Combining the haloallyl ion dissociation enthalpies and allyl halide acidities with the auxiliary data from Table 1 according to eq 7 gives three independent values for the 298 K heat of formation for vinyl carbene, $\Delta H_{f,298}$(CH_2=CHCH): 92.3 $\pm$ 2.6, 93.9 $\pm$ 3.4, and 93.2 $\pm$ 3.1 kcal/mol from the chloride, bromide, and iodide systems, respectively (Table 2). The indicated uncertainties are derived from the root-square sum of the uncertainties in each term in eq 7. The agreement among the three values is excellent; pooling all the data gives a final average value of $\Delta H_{f,298}$(CH_2=CHCH) = 93.3 $\pm$ 3.4 kcal/mol.

Phenylcarbene. The α-halobenzyl anions, $PhCHX^-$, with X = Cl, Br, and I were produced by reaction of OH$^-$ with the corresponding benzyl halides. Halide ions were also observed as primary and secondary reaction products. CID of α-halobenzyl anions with argon target in the 1−10 eV (CM) collision energy range produces the halide ion as the only ionic product (eq 4). Halide ion appearance curves obtained from energy-resolved CID of each the three halobenzyl anions are shown in Figure 4. As with the haloallyl anions, no features due to reactions with O_2 contaminant in the target gas are observed in

(58) The 1-halopropenes are 1−2 kcal/mol lower in energy than the 3-halopropene isomers (ref 5), which means that the 3-position in a 1-haloallyl anion is the thermodynamically preferred site of protonation.

(59) Ervin, K. M.; Gronert, S.; Barlow, S. E.; Gilles, M. K.; Harrison, A. G.; Bierbaum, V. M.; DePuy, C. H.; Lineberger, W. C.; Ellison, G. B. *J. Am. Chem. Soc.* **1990**, *112*, 5750.

(60) Graul, S. T.; Schnute, M. E.; Squires, R. R. *Int. J. Mass Spectrom. Ion Processes* **1990** *96*, 181.

(61) Bartmess, J. E.; McIver, R. T., Jr. In *Gas Phase Ion Chemistry*; Bowers, M. T., Ed.; Academic Press: New York, 1979; Vol. 2, Chapter 11.

(62) Chase, M. W.; Davies, C. A.; Downey, J. R.; Frurip, D. J.; McDonald, R. A.; Syverud, A. N. *J. Phys. Chem. Ref. Data* **1985**, *14*, Suppl. 1 (JANAF Tables).

(63) A concise description of these calculations can be found in ref 56. Note that the first term of eq A2 in this paper contains a minor typographical error, it should read $^5/_2R$ ln(T).

(64) Dahlke, G. D.; Kass, S. R. *J. Am. Chem. Soc.* **1991**, *113*, 5566.

Table 3. Total Energies, Zero-Point Energies, Singlet−Triplet Splitting, Carbene Stabilization Energy, and Heat of Formation for Vinylcarbene[a]

level[b]	E_{tot} $^3A''$	E_{tot} $^1A'$	E_{tot} $^1A''$	$\Delta E(^3A''-{}^1A')$	CSE($^3A''$)[c]	$\Delta H_{f,298}(^3A''$ $CH_2CHCH)$[d]
MCSCF(4,4)/cc-pVDZ	−115.85056	−115.83166	−115.82157	−13.2	17.1	98.4
CISD+DV2/cc-pVDZ	−116.20253	−116.18597	−116.17738	−11.7	17.4	98.1
BVWN5/cc-PVTZ	−117.24293	−117.22630		−11.7	27.3	88.2
B3LYP/cc-pVTZ	−116.62269	−116.60358		−13.3	26.0	89.5
zero-point energy[e]	28.4	29.7	28.3			
$H_{298} - H_0$[e]	3.0	2.7	2.9			
expt					21.4 ± 3.5	93.3 ± 3.4

[a] Total energies in atomic units; all other quantities in kcal/mol. [b] Geometries obtained from MCSCF(4,4)/3-21G optimizations. [c] Equation 11. [d] Equation 12. [e] Derived from ROHF/6-31G* frequencies, scaled by a factor of 0.9.

the CID cross sections. The maximum CID cross sections for the halobenzyl ions are estimated to be 1, 3, and 9 Å^2 for the chloride, bromide, and iodide, respectively.

The average internal energies of the $PhCHX^-$ ions estimated from the calculated vibrational frequencies[31] are 2.5, 2.8, and 3.0 kcal/mol for X = Cl, Br, and I, respectively. Because of the greater number of degrees of freedom and stronger bonds in halobenzyl anions compared to the other two systems, kinetic shifts in the CID onsets are significant. Dissociation probability factors, P_D in eq 5, were obtained by using the RRKM model described in the Experimental Section. Analysis of replicate data sets for each of the halobenzyl anions was carried out with and without the ion dissociation lifetime effects included in the model. Average values for the fitting parameters E_T and n obtained from the analysis including ion dissociation lifetime effects are given in Table 2 for each system. The final uncertainty assigned to each E_T value was determined from the precision of the measurements, a 0.5−0.8 kcal/mol (0.15 eV, lab) uncertainty in the energy scale, and an additional 1 kcal/mol due to the uncertainty in the ion lifetime analysis.[36] The kinetic shifts, determined from the difference between the two values of E_T for each ion obtained with and without inclusion of the ion lifetime effects, amount to 4.6, 1.8, and 1.1 kcal/mol for the chloride, bromide, and iodide systems, respectively. The 298 K enthalpy changes for reaction 4 are determined by applying the appropriate temperature corrections and a *RT* factor to each E_T value.

The gas-phase acidities of the benzyl halides were estimated by the bracketing method. For these systems proton transfer reactions in both directions could be examined without ambiguity since protonation of a α-halobenzyl anion at the α-carbon is strongly preferred. The results of these experiments are summarized in tabular form in the Supporting Information. Benzyl chloride has an estimated acidity (ΔG_{acid}) of 364.9 ± 2.0, lying between that of acetonitrile and 2-fluoroethanol. Benzyl bromide transfers a proton to moderately strong bases such as *t*-BuO^-, cyclopropyl methoxide (ΔG_{acid} (c-$C_3H_5CH_2$-OH) = 367.5 ± 0.5 kcal/mol)[60] and CH_2CN^-, but appears to react only by nucleophilic substitution with F^-. Weaker bases, such as deprotonated 3,3-dimethyl-2-butanol (ΔG_{acid} = 364.5 ± 2.0 kcal/mol)[5] and acetone enolate ($\Delta G_{acid}((CH_3)_2CO)$ = 361.9 ± 2.0 kcal/mol),[5] do not react with benzyl bromide via proton transfer. Bromobenzyl anion abstracts a proton from acetonitrile and from stronger acids, such as 3,3-dimethyl-2-butanol and acetone. From these results, $\Delta G_{acid}(PhCH_2Br)$ of 364.5 ± 2.0 kcal/mol is assigned. Benzyl iodide undergoes proton transfer with $FCH_2CH_2O^-$ and stonger bases, while proton transfer does not appear to take place with 3,3-dimethyl-2-butanol and acetone. Bracketing reactions between iodobenzyl anion and reference acids were difficult to interpret, as only acetone and CF_3CH_2OH reacted with $PhCHI^-$ to give a significant yield of proton transfer product. The other acids either did not react by proton transfer or reacted too slowly to make reliable conclusions. For this reason, the bracketing results obtained from the $PhCH_2I$ reactions were used to assign ΔG_{acid}-($PhCH_2I$) = 364.5 ± 2.0 kcal/mol.

Entropies of ionization, ΔS_{acid}, for the benzyl halides were estimated by using the same procedures used for the allyl halides.[63] Values of 23.7, 24.1, and 24.4 eu were computed for benzyl chloride, bromide, and iodide, respectively. Combining ΔS_{acid} with ΔG_{acid} values gives $\Delta H_{acid}(C_6H_5CH_2X)$ = 372.0 ± 2.0, 371.7 ± 2.0, and 371.8 ± 2.0 kcal/mol for X = Cl, Br, and I, respectively.

Combining the dissociation enthalpies for the halobenzyl ions with the benzyl halide acidities and the auxiliary data from Table 1 according to eq 7 gives values for the 298 K heat of formation for phenyl carbene, $\Delta H_{f,298}(C_6H_5CH)$, of 103.2 ± 3.2, 105.5 ± 2.7, and 100.9 ± 2.8 kcal/mol from the chloride, bromide, and iodide systems, respectively (Table 2). The final uncertainty assigned to each value is the root-square sum of the component uncertainties, which is dominated by the uncertainty in the gas-phase acidity of each benzyl halide. The spread among the three independent measurements (4.6 kcal/mol) is somewhat larger than that obtained for methylene and vinyl carbene, but all the assigned uncertainties overlap. Pooling the data from all measurements gives the final average: $\Delta H_{f,298}(C_6H_5CH)$ = 102.8 ± 3.5 kcal/mol.

Computational Results. Optimized geometries for the triplet ground states ($^3A''$) and the two lowest singlet states ($^1A'$ and $^1A''$) of **1**−**3** were obtained from MCSCF(*n*,*n*)/3-21G calculations, in which the active spaces included the carbon σ orbital and all π-type orbitals in each (planar) molecule. Geometries for the $^3A''$ and $^1A'$ states were also computed with the BVWN5/cc-pVDZ procedure. The structural details will not be discussed here, other than to say that the present calculations give optimal geometries for these carbenes that are consistent with the results of previous computational studies.[12,14,15,17−19] Complete listings of the calculated structural parameters for **1**−**3** and the corresponding hydrocarbons methane, propene, and toluene are provided with the Supporting Information. Total energies for each of these species obtained from MCSCF, CISD, and DFT (BVWN5 and B3LYP) calculations employing either the cc-pVDZ or cc-pVTZ basis set are listed in Tables 3−5, along with the zero-point vibrational energies and 0−298 K integrated heat capacities derived from the scaled harmonic frequencies. The ZPE-corrected energy difference between the lowest singlet and triplet states of **2** and **3**, $\Delta E(^3A'' - {}^1A')$ obtained from the four different approaches, is given in the fifth column of Tables 3 and 4. Theoretical estimates for the heats of formation of phenylcarbene and vinylcarbene were derived from the calculated enthalpy change for the isodesmic reaction shown below (eq 11, R = C_6H_5, CH_2═CH).

$$(^3A'')\ RCH + CH_4 \rightarrow RCH_3 + (^3B_1)\ CH_2 \qquad (11)$$

The energetics of this hypothetical dihydrogen transfer reaction

Table 4. Total Energies, Zero-Point Energies, Singlet−Triplet Splitting, Carbene Stabilization Energy, and Heat of Formation for Phenylcarbene[a]

level[b]	E_{tot} $^3A''$	E_{tot} $^1A'$	E_{tot} $^1A''$	$\Delta E(^3A''-{}^1A')$	CSE($^3A''$)[c]	$\Delta H_{f,298}(^3A''$ PhCH)[d]
MCSCF(8,8)/cc-pVDZ	−268.57088	−268.55693	−268.53507	−10.7	11.0	111.7
CISD+DV2/cc-pVDZ	−269.35972	−269.34846	−269.32486	−9.0	12.8	109.9
BVWN5/cc-pVTZ	−271.68499	−271.67783		−6.4	19.3	103.4
B3LYP/cc-pVTZ	−270.32585	−270.31656		−7.7	17.5	105.2
zero-point energy[e]	62.0	63.9	62.7			
$H_{298} - H_0$[e]	4.2	3.9	4.1			
expt					19.9 ± 3.6	102.8 ± 3.5

[a] Total energies in atomic units; all other quantities in kcal/mol. [b] Geometries obtained from MCSCF(8,8)/3-21G optimizations. [c] Equation 11. [d] Equation 12. [e] Derived from ROHF/6-31G* frequencies, scaled by a factor of 0.9.

Table 5. Total Energies and Zero-Point Energies for $^3B_1$ Methylene, Methane, Propene, and Toluene[a]

level[b]	E_{tot} $^3B_1$ CH_2	E_{tot} CH_4	E_{tot} CH_2=$CHCH_3$	E_{tot} $PhCH_3$
MCSCF(*n*,*n*)/cc-pVDZ[c]	−38.92038	−40.19641	−117.10521	−269.82736
CISD+DV2/cc-pVDZ	−39.02957	−40.35970	−117.51074	−270.66733
BVWN5/cc-pVTZ	−39.39351	−40.79941	−118.61125	−273.05803
B3LYP/cc-pVTZ	−39.16844	−40.53849	−117.95724	−271.66600
zero-point energy[e]	10.5	27.0	48.5	77.4
$H_{298} - H_0$[e]	2.4	2.4	3.1	4.6

[a] Total energies in atomic units; all other quantities in kcal/mol. [b] Geometries obtained from MCSCF(*n*,*n*)/3-21G optimizations. [c] MCSCF(2,2) for methylene, MCSCF(4,4) for propene, MCSCF(8,8) for toluene, HF for methane; see text for descriptions of active orbital spaces. [d] Derived from RHF/6-31G* or ROHF/6-31G* frequencies, scaled by a factor of 0.9.

provide a measure of the stabilization or destabilization imparted by a substituent relative to triplet methylene, and is referred to as the "carbene stabilization enthalpy" or CSE.[2b,65] The heat of formation of RCH can be evaluated by combining the CSE value with the known heats of formation of RCH_3, CH_4, and CH_2 (Table 1) according to eq 12.

$$\Delta H_{f,298}(RCH) = \Delta H_{f,298}(RCH_3) + \Delta H_{f,298}(^3B_1\ CH_2) - \Delta H_{f,298}(CH_4) - CSE \quad (12)$$

Values of the CSE, corrected to 298 K, are given for the triplet states of **2** and **3** in the tables, along with the resulting estimate for $\Delta H_{f,298}$(RCH) obtained from the different theoretical methods.

Discussion

The good agreement between the heat of formation for CH_2 measured in this work and the well-established literature value for $\tilde{X}$ $^3B_1$ CH_2 indicates that dissociation of collisionally-activated CH_2Cl^- and CH_2Br^- ions occurs at the adiabatic limit with an observable threshold that properly reflects the reaction endothermicity. Furthermore, the consistency among the values determined for ΔH_f(**2**) from the three different haloallyl anion experiments strongly suggests that the same C_3H_4 product is formed in each case, and that the haloallyl anion dissociations are also occurring at the thermodynamic limit. Although the variation among the heats of formation for phenylcarbene derived from the three different halides is larger than that for the other two carbenes, it is nonsystematic and the independent values are all within the uncertainty assigned to the final pooled average. We therefore conclude that halide dissociation from each of the activated halobenzyl anions occurs adiabatically to produce the same C_7H_6 product at threshold. These and other factors necessary to evaluate the experimental results are discussed below.

Electron Detachment. In performing energy-resolved CID studies with negative ions, one must recognize the potential complications of collision-induced electron detachment. This could suppress the total cross section for reaction to such an extent that the dissociation onset cannot be observed at the true threshold, resulting in a "competitive shift"[66] of the appearance curve to higher energies. In previous studies of negative ion CID, we concluded that collision-induced electron detachment becomes competitive with dissociation only when the activation energy for the dissociation exceeds the electron detachment energy by a large margin (*ca.* 1 eV).[7,26−28] The chlorocarbanions naturally possess the highest halide dissociation energies for reactions 2−4; therefore, any deleterious effects of collision-induced electron detachment would be greatest with these ions. Estimates of the electron affinities of CH_2Cl, CH_2=$CHCHCl$, and PhCHCl radicals can be derived from the measured acidities and C−H bond energies of the corresponding chlorohydrocarbons according to the following relation: $EA(R) = D(R-H) - \Delta H_{acid}(RH) + IP(H)$. The α-CH bond energies in methyl chloride and allyl chloride are given in the NIST compilation[5] as 100.9 and 88.6 kcal/mol, respectively; for benzyl chloride we estimate a value of 87 kcal/mol. These combine with the appropriate acidities listed in Table 2 to give $EA(CH_2Cl)$ = 14.5 kcal/mol, $EA(CH_2$=$CHCHCl)$ = 26.8 kcal/mol, and EA(PhCHCl) = 22.9 kcal/mol. The measured chloride dissociation energies of CH_2Cl^-, CH_2=$CHCHCl^-$, and $PhCHCl^-$ are 21.9, 28.6, and 37.4 kcal/mol, respectively (Table 2). Thus, the chloride dissociation energy exceeds the electron binding energies of the carbanion in each case, but only by small amounts ranging from about 2 to 15 kcal/mol. The apparent absence of any adverse effects due to electron detachment in the CH_2Cl^- experiments, plus the fact that the maximum CID cross sections measured for all the halocarbanions (1−10 Å^2) are in the "normal" range for negative ion CID,[7,27,28] suggests that competitive shifts in the CID onsets due to collision-induced electron detachment are unimportant.

Product Structures. Since only the ionic products of a CID are observed directly, the identity of the accompanying neutral product must be inferred. Although the corresponding carbenes are the simplest mechanistic alternatives for the products of halide loss from haloallyl and halobenzyl anions, rearrangements to lower energy isomeric forms are conceivable. Note, however, that such rearrangements are relevant only if they take place

(65) Rondan, N. G.; Houk, K. N.; Moss, R. A. *J. Am. Chem. Soc.* **1980,** *102,* 1770.

(66) Lifshitz, C.; Long, F. A. *J. Chem. Phys.* **1964**, *41*, 2468.

during the halide dissociation event that is probed by energy-resolved CID (not afterwards), and only if the activation parameters for the dissociative rearrangements (E_a and $\Delta S^{\ddagger}$) are more favorable than those for simple, direct halide cleavage without rearrangement. Unimolecular decomposition reactions involving hydrogen rearrangements and/or skeletal rearrangements are usually associated with tighter transition states compared to simple bond-cleavage reactions and, as a result, are less efficient unless their activation energies are exceptionally low.[67] The maximum CID cross sections obtained for the haloallyl and halobenzyl anions (3−10 Å^2) are similar in magnitude to those determined for direct-cleavage CID reactions of many other negative ions examined in our laboratory in which rearrangements do not occur.

The stable, closed-shell C_3H_4 isomers are methyl acetylene (ΔH_f = 44.6 kcal/mol),[5] allene (ΔH_f = 45.6 kcal/mol)[5] and cyclopropene (ΔH_f = 66.2 kcal/mol).[5] Yoshimine and co-workers mapped the C_3H_4 potential energy surface using MCSCF and multi-reference CI procedures in conjunction with a polarized, double-ζ basis set.[15] Thermal interconversion among the three isomers noted above is calculated to take place on the singlet surface via rearrangements involving vinylcarbene, cyclopropanylidene (c-$(CH_2)_2$C:), and propenylidene (CH_3-CH=C:) intermediates.[15c] Triplet vinylcarbene is calculated to lie 45.9 kcal/mol higher in energy than methylacetylene,[15a,b] which suggests a heat of formation for this species of 44.6 + 45.9 = 90.5 kcal/mol. This theoretical estimate for ΔH_f(CH_2-CHCH) is in satisfactory agreement with our experimental value (Table 2) and with the values predicted by DFT calculations (*vide infra*). The singlet states of vinylcarbene (^{1}A′), cyclopropanylidene (^{1}A$_1$), and propenylidene (^{1}A′) are predicted to be higher in energy than methylacetylene by 54.0, 62.3, and 42.2 kcal/mol, respectively, suggesting heats of formation of 98.6, 106.9, and 86.8 kcal/mol, respectively.[15c] Singlet vinylcarbene and cyclopropanylidene are therefore ruled out as products of haloallyl anion CID since the experiments indicate a significantly lower value for ΔH_f(C_3H_4). Propenylidene and the three stable, closed-shell C_3H_4 isomers can also be ruled out since the computed transition states for their formation lie 59−66 kcal/mol above that for methyl acetylene (13−20 kcal/mol above triplet vinylcarbene).[15c] It is unlikely that the proximal halide ion in the decomposing [C_3H_4···X^-]* complexes formed during CID could lower these rearrangement barriers by the 11−18 kcal/mol needed to match the experimentally-determined value for ΔH_f(C_3H_4). We therefore conclude that the nascent C_3H_4 product formed at threshold in the haloallyl CID experiments is the unrearranged vinylcarbene in its triplet ground state.

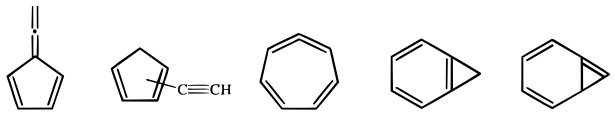

4 **5** **6** **7** **8**

The apparent heat of formation of the C_7H_6 product of halobenzyl anion CID is 101−105 kcal/mol (Table 2). We can therefore rule out the acyclic C_7H_6 isomers, all of which have heats of formation greater than 118 kcal/mol.[48] Lower energy C_7H_6 isomers include fulvenallene (**4**, ΔH_f(est) = 82 kcal/mol),[48] the ethynylcyclopentadienes (**5**, ΔH_f(est) = 90 kcal/mol),[48] 1,2,4,6-cycloheptatetraene (**6**, ΔH_f(est) = 92 kcal/mol),[20−22] benzocyclopropene (**7**, ΔH_f = 89 ± 1 kcal/mol[68]), and bicyclo-[4.1.0]hepta-2,4,6-triene (**8**, ΔH_f(est) = 107 kcal/mol).[21,22] Pyrolysis of phenylcarbene at temperatures in excess of 600 °C leads to the ring-contracted products **4** and **5**, while at lower temperatures ring expansion to **6** occurs.[69,70] Theoretical studies of the C_7H_6 potential energy surface have been carried out by Matzinger *et al.*,[20] Wong and Wentrup,[21] and Schaefer, Schleyer, and Borden.[22] These high-level calculations indicate that cycloheptatetraene **6** is the central intermediate for formation of both the ring-contracted and ring-expanded products **4**−**7**. Moreover, the near-degenerate rearrangement of phenylcarbene to **6** is calculated to occur on the singlet surface *via* the bicyclic triene **8** with an activation barrier of *ca*. 17 kcal/mol. This places the key transition state for isomerization of phenylcarbene to **4**−**8** at about ΔH = 122 kcal/mol—much higher than the apparent enthalpy of the C_7H_6 product of the threshold CID experiments. As stated above for the haloallyl system, it is unlikely that the presence of the halide ion in the activated halobenzyl carbanion complexes would reduce the rearrangement barrier to any significant extent, so we can rule out isomers **4**−**8** as the C_7H_6 product of halobenzyl anion CID. Mechanistic considerations and the measured energetics are most consistent with formation of phenylcarbene.

Gas-Phase Acidities of Methyl, Allyl, and Benzyl Halides. The differing trends in the α-CH acidities of methyl, allyl, and benzyl halides (X = Cl, Br, I) deserve comment. In general, halogen substitution increases α-CH acidity.[71] Sigma electron withdrawal by the electronegative halogen stabilizes the negative ion and induces a greater s-character in the carbanion lone pair, and the destabilizing four-electron π interaction involving the lone pairs of Cl, Br, and I is minimal. Methyl chloride is about 17 kcal/mol more acidic than methane (ΔH_{acid}(CH_4) = 416.6 kcal/mol),[5] while methyl bromide is 22 kcal/mol more acidic. The NIST compilation[5] lists ΔH_{acid}(CH_3I) as 386.4 ± 4.9 kcal/mol, which suggests a 30-kcal/mol increase for iodine substitution. However, this value comes from the same FT-ICR study that gave ΔH_{acid} values for CH_3Cl and CH_3Br that are believed to be too low by 4 kcal/mol.[53] Assuming the same correction for CH_3I gives ΔH_{acid} (CH_3I) = 390 ± 5 kcal/mol. The effect of iodine-substitution on the acidity of methane then becomes 26 kcal/mol. Thus, for the series CH_3X, X = Cl, Br, I, ΔH_{acid} decrements by 5 kcal/mol for each substitution. Replacing a hydrogen in a methyl halide with a vinyl or phenyl group leads to a compression in the differences among the three halocarbons. The allyl halides are more acidic than propene by 15−20 kcal/mol (ΔH_{acid}(propene) = 391.1 ± 0.3 kcal/mol),[72] but in this series the chloride and bromide have identical acidities, while the iodide is more acidic by 4−5 kcal/mol. Moreover, the three benzyl halides have identical ΔH_{acid} values lying about 10 kcal/mol below that for toluene (ΔH_{acid}(toluene) = 382.3 ± 0.5 kcal/mol).[72] The differing trends for the three systems can be understood by considering the charge distributions in the negative ions. Polarization and delocalization of π-electron density by the vinyl and phenyl groups results in diminished electron density at the α-carbon compared to a halomethyl anion, and attenuated differences between the three halides. Compared to vinyl, the larger, more polarizable π-system of a phenyl group

(67) Busch, K. L.; Glish, G. L.; McLuckey, S. A. *Mass Spectrometry/Mass Spectrometry Techniques and Applications of Tandem Mass Spectrometry*; VCH: New York, 1988.

(68) Billups, W. E.; Chong, W. Y.; Leavell, K. H.; Lewis, E. S.; Margrave, J. L.; Sass, R. L.; Shieh, J. J.; Werness, P. G.; Wood, J. L. *J. Am. Chem. Soc.* **1973**, *95*, 7878.

(69) Joines, R. C.; Turner, A. B.; Jones, W. M. *J. Am. Chem. Soc.* **1969,** *91*, 7754.

(70) Schissel, P.; Kent, M. E.; McAdoo, D. J.; Hedaya, E. *J. Am. Chem. Soc.* **1970,** *92*, 2147.

(71) Rodriquez, C. F.; Sirois, S.; Hopkinson, A. C. *J. Org. Chem.* **1992**, *57*, 4869.

(72) Ellison, G. B.; Davico, G. E.; Bierbaum, V. M.; DePuy, C. H. *Int. J. Mass Spectrom. Ion Processes* **1996**, *156*, 109.

leads to a greater attenuation of the absolute and differential halogen-substituent effects.

Dissociation Dynamics. The consistency of the thermochemical results for triplet carbenes **2**−**4** obtained with the different halocarbanion precursors indicates that the obligatory curve-crossings involved in dissociation reactions 2−4 occur at energies below the triplet product asymptotes (Figure 1B), and that intersystem crossing by the activated ions occurs rapidly on the time scale of halide loss. We recently reported some examples of "spin-forbidden" dissociations of another series of halocarbanions in which these same conclusions evidently do not apply.[28] Halide loss from collisionally-activated *o*-, *m*-, and *p*-halobenzyl anions, which are isomers of the α-halobenzyl anions shown in eq 4, yields the (σ,π)-biradicals α,2-, α,3-, and α,4-dehydrotoluene, respectively (e.g., eq 13 shown for the α,4 isomer). α,2- and α,4-dehydrotoluene are ground state triplets (^{3}A″ and ^{3}B$_1$, respectively), whereas the α,3 isomer is a ground state singlet (^{1}A″). The apparent heats of formation derived for the two triplet biradicals displayed a systematic dependence upon the halide precursor, with the chlorides giving the highest and the iodide giving the lowest apparent heats of formation. In contrast, the results for the singlet α,3 biradical were invariant with changes in the halide precursor. Arguments were presented that the halide dependence of the triplet biradical measurements could have resulted from a reverse activation barrier in the *o*- and *p*-halobenzyl anion dissociations (e.g. Figure 1C) that minifies with the iodides. Alternatively, halide-dependent variations in the rate-limiting singlet−triplet intersystem crossing (e.g. Figure 1B with k_{isc}(I) > k_{isc}(Br) > k_{isc}(Cl))

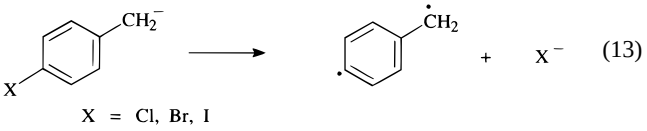

(13)

could also lead to halide−dependent variations in the apparent heats of formation. In the limit of very slow intersystem crossing, diabatic dissociation would occur to produce the higher energy singlet product, while fast intersystem crossing is required for adiabatic dissociation to the triplet. Enhanced rates of intersystem crossing are expected for the iodides and bromides due to heavy-atom induced spin−orbit coupling.[73]

The presence of a systematic halide effect in the triplet biradical experiments and its absence in the triplet carbene measurements can be rationalized by considering the nature of the lowest singlet states in the two systems. For carbenes **1**−**3** the lowest singlet state is "closed-shell" with the $\sigma^2\pi^0$ configuration predominating,[12,14,15,19−22] whereas for α,2- and α,4-dehydrotoluene the "open shell" singlet with a $\sigma^1\pi^1$ configuration is the lowest singlet state.[28] As dissociation of an activated halocarbanion proceeds, the lowest singlet configuration of the nascent carbene or biradical will dominate the evolving mixture of configurations that exists prior to singlet−triplet intersystem crossing. In the region of the crossing on the potential energy surface, transitions between the singlet $\sigma^2\pi^0$ and triplet $\sigma^1\pi^1$ configurations of the carbenes are spin−orbit allowed, whereas transitions between the singlet $\sigma^1\pi^1$ and triplet $\sigma^1\pi^1$ configurations of the biradicals are spin−orbit forbidden because the singlet−triplet electronic transition does not involve a change in orbital angular momentum.[74] Therefore, the intersystem crossing rates are generally greater in the carbene-forming dissociations than in the biradical-forming dissociations and, as a result, systematic halide effects are not observed in the former processes.

Calculated Energetics. The predicted CSE values and heats of formation for **2** and **3** given by the four different levels of theory indicated in Tables 3 and 4 differ significantly. In general, the MCSCF and CISD+DV2 calculations predict *ca.* 10 kcal/mol smaller carbene stabilizations and correspondingly higher heats of formation than the two DFT procedures. For vinyl carbene, the absolute heats of formation predicted by the MCSCF and CISD+DV2 calculations are higher than the experimental value by 5 kcal/mol. A similar discrepancy between experiment and these same levels of theory was found previously in the α,*n*-dehydrotoluene study.[28] Both DFT-derived estimates are too low compared to experiment by 3−5 kcal/mol, but close to the value for ΔH_f[^{3}A″ CH$_2$═CHCH] derived from the MRCI/DZP calculations reported by Yoshimine and co-workers.[15]

For phenylcarbene, the disparity among the heats of formation computed by the different methods is 7 kcal/mol, but in this case the DFT predictions are in good agreement with experiment. Using the experimental heat of formation of benzocyclopropene (89 ± 1 kcal/mol)[68] in conjunction with the computed C$_7$H$_6$ isomer energy difference reported by Wong and Wentrup[21] suggests heats of formation for phenylcarbene of 108.1 and 104.9 kcal/mol at the G2(MP2,SVP) and BLYP/6-311+G(3df,2p) levels of theory, respectively. Semiempirical methods predict heats of formation for ^{3}A″ phenylcarbene in the 98−111 kcal/mol range,[18] with the AM1 results (102.9 kcal/mol)[18] showing the best agreement with experiment.

The variation in the singlet−triplet splittings computed by the different methods are smaller. For comparison, the calculated ($\tilde{X}$ ^{3}B$_1$ → $\tilde{a}$ ^{1}A$_1$) splittings for methylene at the MCSCF, CISD+DV2, BVWN5, and B3LYP levels of theory are −11.6, −12.1, −9.7, and −11.0 kcal/mol, respectively (experimental ΔE_{ST} = 9.0 kcal/mol).[10] At the MCSCF and CISD+DV2 levels of theory, the "open-shell" ^{1}A″ state of vinylcarbene is calculated to lie 5−6 kcal/mol above the lowest singlet state, whereas for phenylcarbene the ($\tilde{a}$ ^{1}A$_1$ → $\tilde{b}$ ^{1}A″) splitting is more than twice as big (14−15 kcal/mol).

Sequential C−H Bond Strengths in Propene and Toluene. The experimental heats of formation for **2** and **3** can be used in conjunction with eq 14 and the thermochemical data listed in Table 1 to derive estimates for the α-CH bond dissociation enthalpies in allyl and benzyl radicals, respectively. The derived

$$RCH_2 \rightarrow RCH + H \qquad (14)$$

$$DH_{298}[RCH-H] = \Delta H_{f,298}(RCH) + \Delta H_{f,298}(H) - \Delta H_{f,298}(RCH_2)$$

values are indicated in Figure 5 along with the CH bond enthalpies of propene and toluene and, for comparison, the corresponding values for methane and methyl radical. The "second" α-CH bond strengths in propene and toluene are the same, within error, and both are approximately 15 kcal/mol larger than the first. The bond strength reductions in propene and toluene relative to methane are well understood manifestations of π-delocalization in the allyl and benzyl radicals.[72,75] The α-CH bonds in allyl and benzyl radicals are found to be 5−6 kcal/mol weaker than the CH bond in methyl radical. The origins of this difference are not readily apparent. When π-delocalization effects are removed, vinyl and phenyl substituents have little or no net effect on the CH bond strength of methane. This can be shown by adding the known CH$_2$

(73) Turro, N. J. *Modern Molecular Photochemistry*, Benjamin/Cummings Publishing Co.: Menlo Park, CA, 1978; Chapter 7.

(74) Salem, L.; Rowland, C. *Angew. Chem., Int. Ed. Engl.* **1972**, *11*, 92.

(75) Hrovat, D. A.; Borden W. T. *J. Phys. Chem.* **1994**, *98*, 10460.

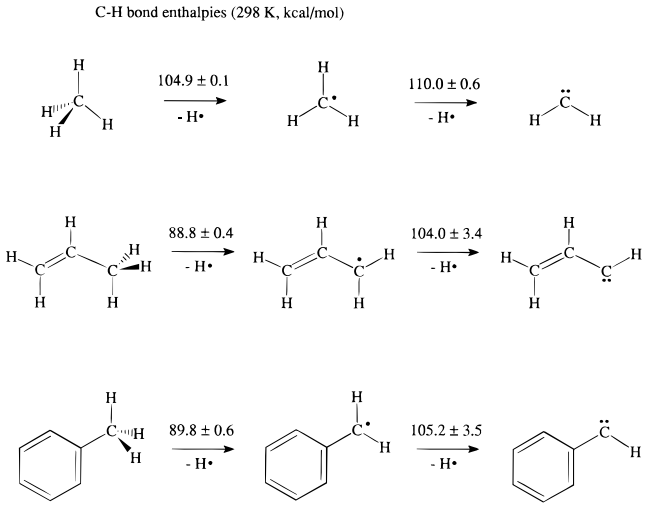

Figure 5. Summary of sequential C−H bond dissociation enthalpies of methane, propene, and toluene.

rotational barriers of allyl radical (15.7 kcal/mol)[76] and benzyl radical (12.5 kcal/mol)[75,74] to the CH bond strengths of propene and toluene, respectively, in order to derive the energy changes for dissociation to the non-conjugated radicals. The resulting bond strengths are about the same as $DH_{298}[CH_3-H]$. Furthermore, the local geometries about the carbene carbon in the triplet states of **1**, **2**, and **3** are similar, with calculated RCH bond angles of 134 ± 1°.

Summary

In this work we have demonstrated the applicability of energy-resolved collision-induced dissociation of α-halocarbanions to the determination of absolute heats of formation for carbenes with triplet ground states. The CID thresholds and acid−base measurements for chloromethyl and bromomethyl anions give a consistent heat of formation for CH_2 (92.2 ± 3.7 kcal/mol) that is in excellent agreement with the well-established literature value for this archetypal triplet carbene (92.9 ± 0.6 kcal/mol).[10,11] This indicates that the formally spin-forbidden dissociation of these carbanions occurs without any significant reverse activation energy, and that the obligatory singlet−triplet intersystem crossing must be rapid on the time scale of halide loss. Three independent measurements each of the absolute heats of formation of the C_3H_4 and C_7H_6 products of Cl^-, Br^-, and I^- loss from α-haloallyl and α-halobenzyl anions were carried out. The two sets of results show good internal consistency, which further validates the thermochemical model for the CID threshold measurements. Thermodynamic and kinetic arguments are presented for identifying the threshold products of α-haloallyl and α-halobenzyl anion CID as vinylcarbene and phenylcarbene, respectively. The measured heat of formation for vinylcarbene, 93.3 ± 3.4 kcal/mol, falls in the middle of the range of values predicted by ab initio and DFT calculations (88−98 kcal/mol). For $\Delta H_{f,298}$(PhCH), the DFT predictions (103−105 kcal/mol) are in good agreement with the experimental heats of formation, 102.8 ± 3.5 kcal/mol, while the values derived from MCSCF and CISD+DV2 methods are 7−9 kcal/mol too high. The measured heats of formation for vinylcarbene and phenylcarbene are used to derive the α-CH bond dissociation energies in allyl and benzyl radicals: $DH_{298}[CH_2CHCH-H]$ = 104.0 ± 3.4 kcal/mol and DH_{298}-[PhCH−H} = 105.2 ± 3.5 kcal/mol.

Acknowledgment. This paper is dedicated to Dr. Marvin Poutsma on the occasion of his 60th birthday. This work was supported by the National Science Foundation and the Department of Energy, Office of Basic Energy Science. We are grateful to Professor Chris Cramer for helpful advice and for sharing theoretical results in advance of publication and to Professor Curt Wentrup for an advance copy of the paper cited in ref 21.

Supporting Information Available: Listing of calculated geometries for molecules in Tables 3−5 and acid−base bracketing results for benzyl halides and allyl halides (6 pages). See any current masthead page for ordering and Internet access instructions.

JA963918S

(76) Korth, H.-G.; Trill, H.; Sustmann, R. *J. Am. Chem. Soc.* **1981**, *103*, 4483.